CHEMISTRY OF MATERIALS
Article

Chem. Mater. **2009,** *21,* 5601–5606 5601
DOI:10.1021/cm901774v

Low Temperature Chemical Vapor Deposition of Hafnium Nitride–Boron Nitride Nanocomposite Films

Navneet Kumar,[†,§] Wontae Noh,[‡,§] Scott R. Daly,[‡,§] Gregory S. Girolami,*[,‡,§] and John R. Abelson*[,†,§]

[†]*Department of Materials Science and Engineering, University of Illinois at Urbana–Champaign, 1304 W. Green Street, Urbana, Illinois 61801,* [‡]*Department of Chemistry, University of Illinois at Urbana–Champaign, 600 South Mathews Avenue, Urbana, Illinois 61801, and* [§]*Frederick Seitz Materials Research Laboratory, 104 South Goodwin Avenue, Urbana, Illinois 61801*

Received June 24, 2009. Revised Manuscript Received October 14, 2009

Nanocomposite HfN_x-BN thin films are deposited by chemical vapor deposition at substrate temperatures of 350–800 °C using the single-source precursor hafnium borohydride, $Hf(BH_4)_4$, in combination with ammonia, NH_3. Below 350 °C, the product is metallic HfB_2 with essentially no incorporation of nitrogen. However, the presence of ammonia decreases the HfB_2 deposition rate considerably; this growth suppression effect is attributed to blocking of reactive surface sites by adsorbed ammonia molecules. At substrate temperatures above 350 °C, film deposition occurs; however, the HfB_2 phase is completely absent. The resulting film stoichiometry is $HfB_yN_{2.5}$; although the value of y is difficult to determine precisely, it is about unity. X-ray photoelectron spectroscopy (XPS) analysis detects Hf–N and B–N bonds *but no Hf–B bonds*; thus the films are nanocomposites that consist of a mixture of hafnium nitride, HfN_x with $x > 1$ and boron nitride. The deposited films are X-ray amorphous and Raman inactive. Compared to HfB_2 films grown under similar precursor pressure and substrate temperature, the HfN_x-BN films are smoother and have a denser microstructure. The thermal activation energy for growth of HfN_x/BN in the reaction-rate limted regime is ~0.72 eV (70 kJ/mol), a value 0.3 eV larger than that for the growth of HfB_2 from $Hf(BH_4)_4$ alone. This difference in activation energy indicates that growth is governed by a different rate-limiting step; we interpret that the $Hf(BH_4)_4$ precursor reacts with ammonia on the growth surface to generate species with Hf–N and B–N bonds, which subsequently lose H_2 and BH_y to generate the nanocomposite. The HfN_x/BN films have resistivities ~10 Ω·cm. Optical transmission and spectroscopic ellipsometry measurements indicate a bandgap of ~2.6 eV.

Introduction

Nanocomposite materials often exhibit enhanced properties owing to synergistic interactions among their component phases, and as a result such materials have great technological potential. Particularly interesting are nanocomposites that combine materials with vastly different electrical, mechanical, optical, magnetic, thermal, structural, or rheological properties. Here, we describe the preparation of ceramic nanocomposite thin films by low temperature chemical vapor deposition.

The transition metal diborides TiB_2, ZrB_2, and HfB_2 are line compounds with the hexagonal AlB_2 structure and high metallic conductivities.[1] In contrast, the corresponding transition metal nitrides TiN, ZrN, and HfN have wide phase fields with the cubic NaCl structure, and their electrical conductivities depend sensitively on stoichiometry. When substoichiometric in nitrogen, they are highly metallic; when overstoichiometric, they are either poor metals (TiN_x) or insulators with bandgaps of 2–3 eV (ZrN_x, HfN_x).[1–3] The most nitrogen-rich materials in the composition field are cubic M_3N_4 phases with the Th_3P_4 structure and closely related materials of stoichiometry $MN_{1.35}$ with the NaCl structure; these phases are insulating with bandgaps of 2.5 eV for Hf_3N_4[1,4,5] and 2.7 eV for $HfN_{1.35}$.[6,7]

There have been a few studies of ternary metal–boron–nitrogen materials, MB_xN_y. Sputtering MB_2 targets in an Ar/N_2 atmosphere affords a mixture of the phases MB_2, MN, and BN, where M is Hf and Ti.[8,9] Chemical vapor deposition (CVD) from a mixture of MCl_4, BCl_3, N_2, and H_2 at substrate temperatures of 850–1350 °C affords a similar mixed phase product

*Corresponding authors. E-mail: girolami@scs.uiuc.edu (G.S.G.); abelson@mrl.uiuc.edu (J.R.A.).

(1) Williams, W. S. *JOM-J. Miner. Met. Mater. Soc.* **1997**, *49*, 38–42.
(2) Aron, P. R.; Grill, A. *Thin Solid Films* **1982**, *96*, 87–91.
(3) Yee, D. S.; Cuomo, J. J.; Frisch, M. A.; Smith, D. P. E. *J. Vac. Sci. Technol. A-Vac. Surf. Films* **1986**, *4*, 381–387.
(4) Von Juza, R.; Rabenau, A.; Nitschke, I. *Z. Anorg. Allg. Chem.* **1964**, *332*, 1–4.
(5) Zerr, A.; Miehe, G.; Riedel, R. *Nat. Mater.* **2003**, *2*, 185–189.
(6) Fix, R.; Gordon, R. G.; Hoffman, D. M. *Chem. Mater.* **1991**, *3*, 1138–1148.
(7) Hoffman, D. M. *Polyhedron* **1994**, *13*, 1169–1179.
(8) Baker, M. A.; Mollart, T. P.; Gibson, P. N.; Gissler, W. *J. Vac. Sci. Technol. A-Vac. Surf. Films* **1997**, *15*, 284–291.
(9) Gissler, W. *Surf. Interface Anal.* **1994**, *22*, 139–148.

© 2009 American Chemical Society
Published on Web 11/02/2009

MB_xN_y (M = Ti, Zr).[10,11] In some cases, the stoichiometry and distribution of local phases (M−B, M−N, and B−N) are a function of the growth conditions, which affords a means to enhance the mechanical properties.[9] Our group reported the deposition of MB_xN_y films at 300 °C by CVD using the hafnium borohydride precursor $Hf(BH_4)_4$ in the presence of nitrogen atoms generated by a remote microwave N_2 plasma.[12] The films contain the phases HfB_2, HfN, and BN, remain amorphous after high temperature annealing and can be used to synthesize multilayer HfB_2/HfB_xN_y hard coatings whose hardness and elastic modulus can be adjusted over a wide range.[12]

Thermal CVD from the $Hf(BH_4)_4$ precursor affords metallic HfB_2 thin films in the temperature range 200−1300 °C.[13,14] Here, we show that CVD from $Hf(BH_4)_4$ in the presence of ammonia at temperatures above 350 °C changes the reaction pathway completely: no HfB_2 is generated—indeed, no Hf−B bonds are present at all; instead, the films consists of a mixture of amorphous HfN_x ($x > 1$) and BN phases. The spectroscopic, electrical, and optical properties of these films are reported in detail.

Experiment

Chemical vapor deposition is carried out in a UHV system[15] with a base pressure of 10^{-8} torr, most of which is hydrogen. The solid $Hf(BH_4)_4$ precursor sublimes with a remarkably high vapor pressure of ~15 torr at room temperature. Before film growth, the flow of $Hf(BH_4)_4$ is adjusted by means of a needle valve so that the precursor pressure inside the chamber was 0.1 mTorr; no carrier gas is used. Ammonia (15 sccm) is delivered to the chamber through a mass flow controller. The total pressure (ammonia + precursor) before initiation of film growth is 0.8 mtorr as measured by a capacitance manometer. Film thickness and microstructure are analyzed ex situ from fracture cross-sectional images on a scanning electron microscope. Growth rates are measured by dividing the scanning electron microscopy (SEM) thickness by the growth time. The growth kinetics and optical dielectric properties of the films are also monitored in situ using spectroscopic ellipsometry (SE) in the energy range 0.75−5.0 eV. For these experiments, as well as for postgrowth determination of the optical constants, the substrate is highly doped silicon that is dipped in hydrofluoric acid to remove the native oxide before loading into the system. To interpret the SE data, the surface roughness is modeled using the Bruggeman effective medium approximation (EMA) as an isotropic composite consisting of 50% film and 50% void, which is a standard model assumption.[16,17] The optical dielectric response of the HfN_x-BN nanocomposite is modeled using the Tauc−Lorentz (TL) model given by

$$\varepsilon_{2\mathrm{TL}}(E) = \left[\frac{AE_oC(E-E_g)^2}{(E^2-E_o{}^2)^2+C^2E^2}\cdot\frac{1}{E}\right],\ \text{for } E > E_g \\ = 0,\ \text{for } E \le E_g \quad (1)$$

where ε_{2TL} is the imaginary part of the dielectric function, A is the fit parameter with unit of energy, E_0 is the peak transition energy, C is the peak broadening, and E_g is the bandgap.[18] The real part of the dielectric constant in this model is calculated by the Kramers−Kronig integral.[18] The pseudodielectric constants $\langle\varepsilon_1\rangle$ and $\langle\varepsilon_2\rangle$ extracted from this procedure fit the data with a mean square error of 5, which is well within the acceptable limit. The model affords the refractive index n and the extinction coefficient k of a bulk film with no surface roughness layer. For an amorphous semiconductor, the bandgap E_g is determined from the extrapolated intercept of the absorbance $\alpha = 4\pi k/\lambda$ with the $h\nu$ axis on a Tauc plot, $(\alpha h\nu)^{1/2}$ vs $h\nu$.[19]

For optical transmission measurements, films are grown on Corning 7059 glass, and the normalized absorbance is calculated from $\alpha = \log(T/T_o)$ where T is the transmittance of the substrate/film combination, and T_0 was the transmittance of the glass substrate alone The absorbances calculated in this way are approximate because they ignore the wavelength-dependent reflectivity of the films; nevertheless, this simplified approach is sufficient to afford an estimate of the bandgap.

For ex situ electrical measurements, the substrate is thermally grown SiO_2 (300 nm) on Si. After film deposition, two parallel strips of aluminum (~100 nm thick) are evaporated onto the surface to enable coplanar resistivity measurements across the gap between the electrodes; the applied bias (> 10 V) is large compared to the potential drop due to the nonohmic contacts; hence, the measurement reveals the bulk resistivity of the film.

Film crystallinity and composition are determined by ex situ X-ray diffraction (XRD; Philips X'pert 2), X-ray photoelectron spectroscopy (XPS; Kratos Axis ULTRA XPS), and Rutherford Backscattering Spectroscopy (RBS) (High Voltage Engineering Van de Graaff), respectively. RBS is also used to measure the atomic density of Hf in the films. The XPS studies are conducted without sputtering in order to avoid atomic mixing and preferential removal of low atomic mass species that make accurate phase identification unreliable.[20]

Results and Discussion

1. Deposition of Films from $Hf(BH_4)_4$ and NH_3. At temperatures below 350 °C, passage of a mixture of $Hf(BH_4)_4$ and ammonia over Si, SiO_2, or glass substrates produces pure HfB_2 films, with relatively little incorporation of ammonia (< 5 at % N). As monitored by SE, the growth rate at 250 °C decreases with increasing ammonia pressure as GR [nm/min] = $16/(1 + 250p_{\mathrm{ammonia}}$ [mtorr]). Thus, in this low temperature regime *ammonia acts as a very effective growth suppressor* for the chemical vapor deposition of HfB_2; at ammonia pressures near 1 mtorr, growth is essentially arrested. We have shown elsewhere, both experimentally and theoretically, that growth

(10) Holzschuh, H. *Thin Solid Films* **2004**, *469*, 92–98.
(11) Peytavy, J. L.; Lebugle, A.; Montel, G. *Wear* **1979**, *52*, 89–94.
(12) Jayaraman, S.; Gerbi, J. E.; Yang, Y.; Kim, D. Y.; Chatterjee, A.; Bellon, P.; Girolami, G. S.; Chevalier, J. P.; Abelson, J. R. *Surf. Coat. Technol.* **2006**, *200*, 6629–6633.
(13) Jayaraman, S.; Yang, Y.; Kim, D. Y.; Girolami, G. S.; Abelson, J. R. *J. Vac. Sci. Technol. A* **2005**, *23*, 1619–1625.
(14) Yang, Y.; Jayaraman, S.; Kim, D. Y.; Girolami, G. S.; Abelson, J. R. *J. Cryst. Growth* **2006**, *294*, 389–395.
(15) Jayaraman, S.; Klein, E. J.; Yang, Y.; Kim, D. Y.; Girolami, G. S.; Abelson, J. R. *J. Vac. Sci. Technol. A* **2005**, *23*, 631–633.
(16) Aspnes, D. E. *Proc. Soc. Photo-Opt. Instrument. Eng.* **1984**, *452*, 60–70.
(17) Schmid, P. E.; Sunaga, M. S.; Levy, F. *J. Vac. Sci. Technol. A-Vac. Surf. Films* **1998**, *16*, 2870–2875.
(18) Jellison, G. E.; Modine, F. A. *Appl. Phys. Lett.* **1996**, *69*, 371–373.
(19) Tauc, J.; Grigorovici, R.; Vancu, A. *Phys. Status Solidi* **1966**, *15*, 627–637.
(20) Hofmann, S. *Prog. Surf. Sci.* **1991**, *36*, 35–87.

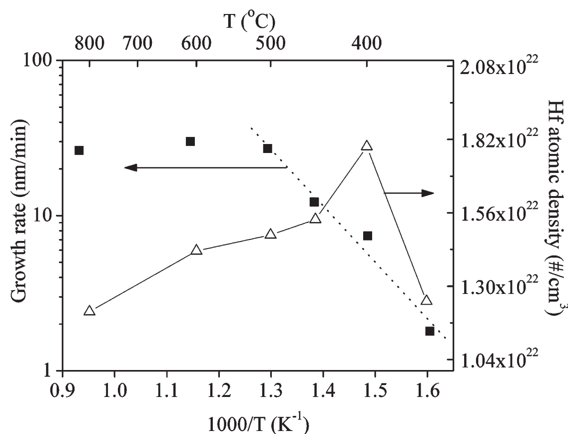

Figure 1. Log of film growth rate (left axis, closed squares) and Hf atomic density from RBS (right axis, open triangles) vs inverse temperature. The low-temperature, reaction-limited regime (dotted line) affords the apparent activation energy.

suppression enhances the conformal coverage of films inside deep trench and via structures.[21,22]

For an ammonia pressure of 1 mtorr, as the substrate temperature is raised, the suppression effect is eventually overcome and film growth occurs. The onset temperature for film growth under these conditions is 350 °C, but there are very long nucleation delays (> 5 min) below substrate temperatures of 450 °C on Si substrates and 500 °C on SiO_2 substrates. To deposit films at temperatures between 350 and 400 °C, it is advantageous to deposit a nucleation layer at 450 °C, then lower the substrate temperature to the desired value. As we will describe below, films grown above 350 °C contain nitrogen and consist of a mixture of hafnium nitride, HfN_x ($x > 1$) and boron nitride, BN. The atomic density of Hf in the films varies from 1.3 to 1.8×10^{22} cm^{-3} and reaches a maximum at 400 °C (Figure 1). For comparison, the theoretical atomic density of Hf in bulk HfN assuming a cell constant of 4.52 Å is 4.2×10^{22} cm^{-3}.[23]

Similar to other CVD processes, the growth rate is reaction rate limited at low temperatures (350−500 °C) and flux limited at high temperatures (Figure 1). The apparent activation energy in the reaction rate limited regime is ~70 kJ/mol (0.72 eV), which is 1.7 times higher than for thermal decomposition of $Hf(BH_4)_4$ alone.[13] This result implies that the rate-limiting step for film growth is different in the presence of ammonia. We suggest that the higher activation energy is due to the formation of Hf-NH_2 species on the surface, which decompose to produce the HfN_x phase in the films. This suggestion is supported by studies of the solution-phase reaction of the analogous molecule $Zr(BH_4)_4$ with ammonia, which affords adducts of stoichiometry $Zr(BH_4)_4(NH_3)_n$, where $n = 4$, 6, or 8.[24] These adducts decompose near room temperature to form ammonium borohydride, NH_4BH_4, and zirconium complexes thought to contain Zr−NH_2 bonds. At higher temperatures, these species evolve H_2 to give an X-ray amorphous solid, which crystallizes above 1000 °C to give a mixture containing ZrN and BN. Similarly, the reaction of the halide precursors ZrX_4 (X = Cl, Br) with ammonia generates a complex $ZrX_4(NH_3)_n$ that affords cubic Zr_3N_4 when annealed.[4]

2. Film Composition. XPS analysis is used to identify phases present on the surface of the film. Often sputtering is used to eliminate the surface oxide on air-exposed samples. We avoid sputtering because it results in atomic mixing and preferential removal of low atomic mass species, which makes accurate phase identification difficult (impossible). XPS analysis of air-exposed films reveals significant differences between films deposited below 350 °C and those deposited above this temperature (Figure 2). For the low temperature films, the Hf 4f ($4f_{5/2}$ and $4f_{7/2}$) region shows features for Hf−O and Hf−B phases, but no features for Hf−N species. The results are consistent with the growth of HfB_2 films followed by surface oxidation upon air exposure. The Hf−B feature is absent for films deposited at higher temperature. Instead, peaks corresponding to Hf−N and Hf−O phases overlap with one another and also with the N 2s peak at 16.7 eV.[25] The shoulder in the 4f peak at ~16 eV arises due to Hf−N bonding and its magnitude indicates that the N/Hf ratio is greater than one.[26] These results support the conclusion that CVD using $Hf(BH_4)_4$ and NH_3 above 350 °C affords composite films containing HfN_x ($x > 1$) and BN phases. The area under B and Hf XPS peaks from the film surface are integrated to obtain the B:Hf ratio of 1.2.

Both the HfB_2 and HfN_x-BN films show a B(1s) peak at 192.25 eV corresponding to B_2O_3 (Figure 3, deconvoluted in panel b). In the HfN_x-BN film, the absence of a B(1s) peak at 187.6 eV indicates the absence of HfB_2; instead, a peak at 190.30 eV indicates the presence of BN.[8,27] RBS analysis of a film deposited at 450 °C on Si (Figure 4) provides a quantitative measure of the film stoichiometry as $HfB_yN_{2.5}$; the boron content y cannot be determined accurately because the boron signal is superposed on the large background due the Si substrate. This result is consistent with the conclusion from the XPS results that the film is composed of HfN_x ($x > 1$) and BN phases.

3. Electrical and Optical Properties. At room temperature, the HfN_x-BN films are highly resistive ($\rho = 12$ Ω-cm), in sharp contrast with HfB_2 films, which are metallic ($\rho \leq 4 \times 10^{-4}$ Ω·cm). The high resistivity is due to the insulating nature of the HfN_x and BN phases. (In comparison, CVD grown $HfN_{1.35}$ reported by Fix et al. were insulators with resistivity > 1 Ω·cm^6 and those

(21) Kumar, N.; Yanguas-Gil, A.; Daly, S. R.; Girolami, G. S.; Abelson, J. R. *J. Am. Chem. Soc.* **2008**, *130*, 17660–17661.
(22) Yanguas-Gil, A.; Yang, Y.; Kumar, N.; Abelson, J. R. *J. Vac. Sci. Technol. A* **2009**, *27*(5), 1244–48.
(23) Johansson, B. O.; Sundgren, J. E.; Helmersson, U.; Hibbs, M. K. *Appl. Phys. Lett.* **1984**, *44*, 670–672.
(24) Kravchenko, O. V.; Kravchenko, S. E.; Polyakova, V. B.; Makhaev, V. D.; Borisov, A. P.; Semenenko, K. N. *Koor. Khim.* **1982**, *8*, 1650–1654.
(25) Perry, A. J.; Schlapbach, L. *Solid State Commun.* **1985**, *56*, 837–841.
(26) Perry, A. J.; Schlapbach, L.; Sproul, W. D. *Solid State Commun.* **1987**, *62*, 23–26.
(27) Panayiotatos, Y.; Logothetidis, S.; Handrea, M.; Kautek, W. *Diam. Relat. Mat.* **2003**, *12*, 1151–1156.

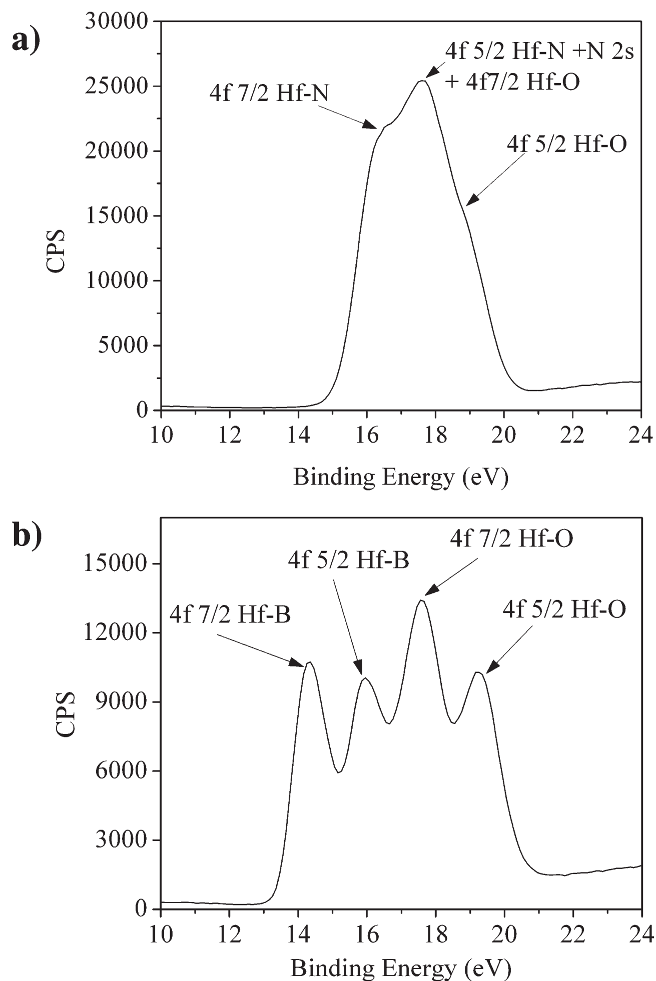

Figure 2. (a) Hf 4f XPS spectrum of the HfN_x-BN film surface. (b) Hf 4f XPS spectrum of the HfB_2 film surface. Arrows identify peak positions as reported in literature references (text).

obtained from sputtering Hf in N_2 atmosphere by Smith had the highest obtained value of 10 $\Omega\cdot$cm[28]).

Ellipsometric analysis of the HfN_x-BN films grown at 450 °C indicates a bandgap $E_g \sim 2.8$ eV (Figure 5). The bandgap estimated from the optical transmission spectrum (Figure 6a) suggests $E_g \sim 2.6$ eV (Figure 6b). The value of bandgap obtained from both methods is close to the range 2.5−2.7 eV reported for CVD Hf_3N_4 films[6,7] and for sputtered HfN_x films[3] but is smaller than of the range 3.6−7.1 eV observed for BN.[29,30] As expected, the properties of the HfN_x-BN films are dominated by the HfN_x component because it has a smaller optical bandgap and higher electrical conductivity than the BN component.

4. Microstructure and Crystallinity. SEM fracture cross sections of a HfN_x-BN film grown at 450 °C reveal a relatively smooth and homogeneous film microstructure (Figure 7a). In contrast, deposition from $Hf(BH_4)_4$ alone at the same temperature yields a very rough and columnar HfB_2 film microstructure.[13] This difference in

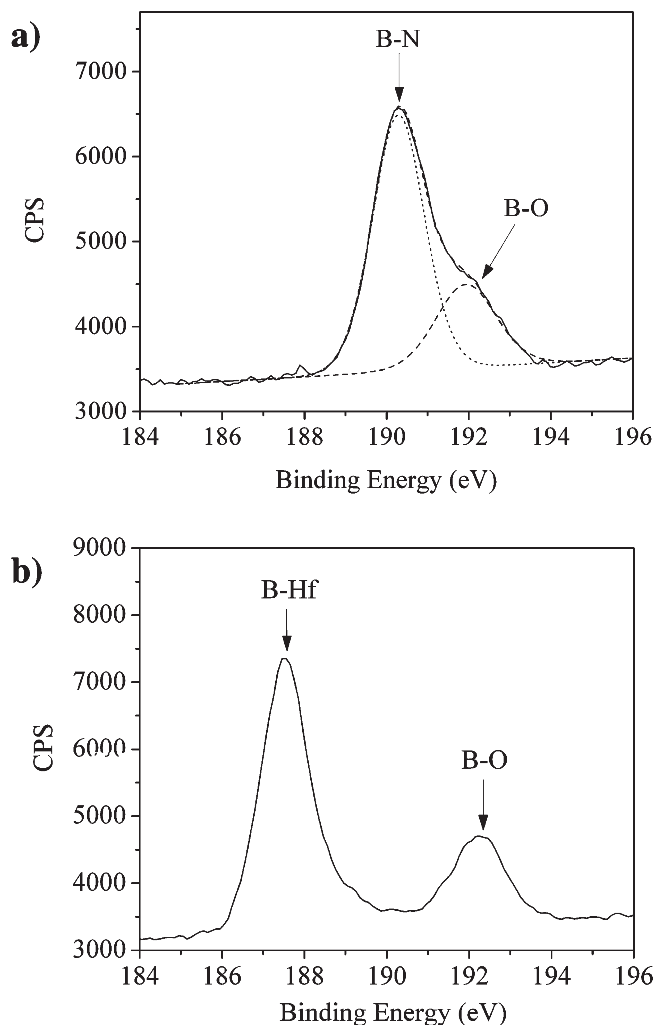

Figure 3. (a) B 1s XPS spectrum (solid line) of the HfN_x-BN film surface. The peaks are deconvoluted using two Gaussians (dashed lines) that correspond to the known oxide and nitride peaks. (b) B 1s XPS spectrum of the HfB_2 film surface.

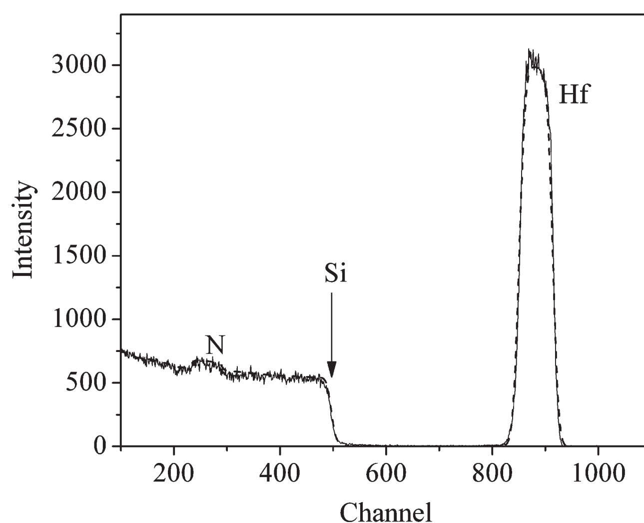

Figure 4. RBS spectrum (dotted line) and model fit (continuous line) of a HfN_x-BN film.

microstructure is consistent with a smaller reactive sticking probability (β) of the $Hf(BH_4)_4$ precursor when excess ammonia is present (ammonia pressures used in our

(28) Smith, F. T. J. *J. Appl. Phys.* **1970**, *41*, 4227.
(29) Watanabe, K.; Taniguchi, T.; Kanda, H. *Nat. Mater.* **2004**, *3*, 404–409.
(30) Zunger, A.; Katzir, A.; Halperin, A. *Phys. Rev. B* **1976**, *13*, 5560–5573.

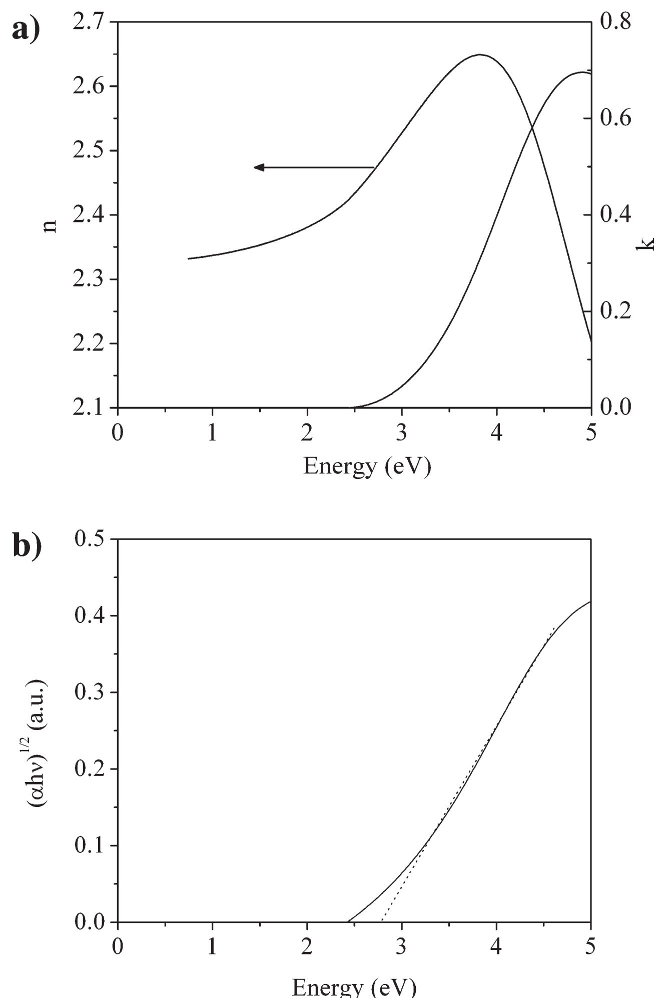

Figure 5. (a) Bulk optical constants n and k for a HfN_x-BN film grown on silicon at 450 °C obtained from ellipsometry data using a Tauc−Lorentz model. (b) Tauc plot, $(\alpha h\nu)^{1/2}$ vs photon energy $h\nu$. The extrapolated linear region (dotted line) intercepts the $h\nu$ axis at the value of the effective bandgap.

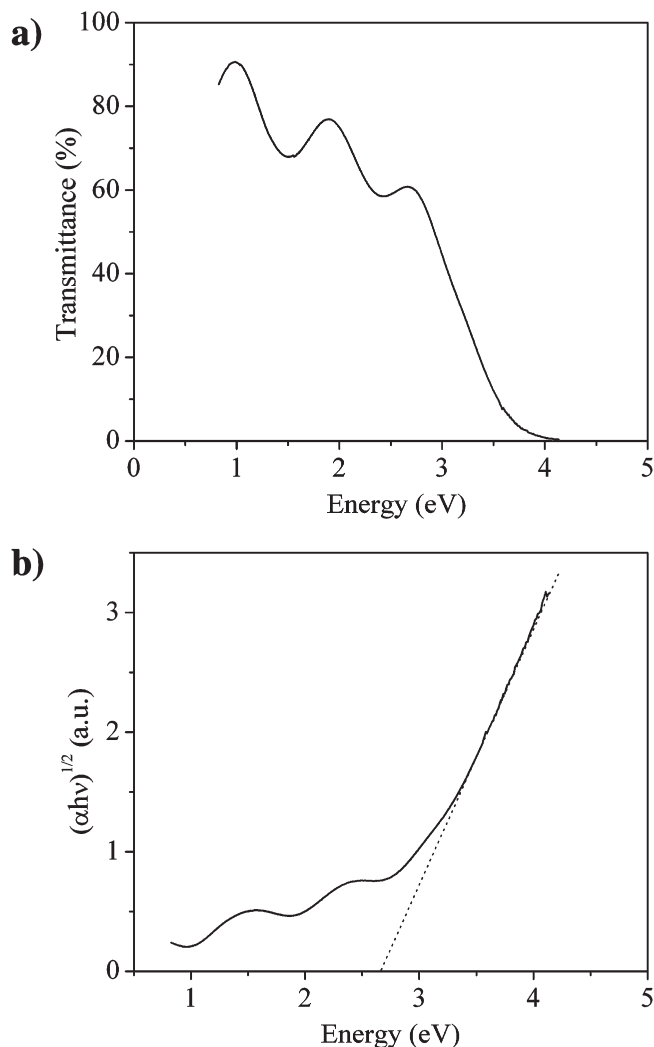

Figure 6. (a) Optical transmittance (solid line) of a HfN_x-BN film grown on Corning 7059 glass at 500 °C. The plot is normalized to the transmission of a bare substrate. (b) Tauc plot (as in Figure 5b).

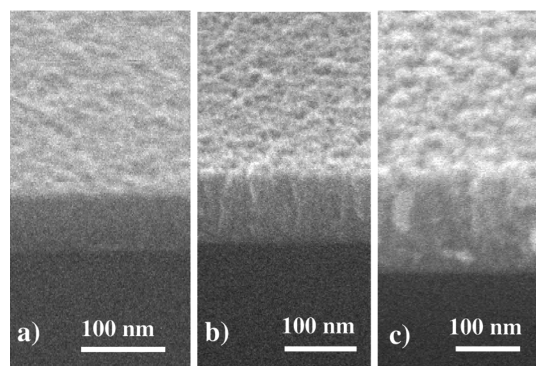

Figure 7. SEM fracture cross sections of HfN_x-BN films grown at (a) 400, (b) 600, and (c) 800 °C on Si substrates.

experiments are 10 times higher than $Hf(BH_4)_4$ precursor pressure). Excess ammonia aids in blocking surface sites for $Hf(BH_4)_4$ adsorption thereby reducing β. A lower β has been shown theoretically[31,32] to afford a smoother surface, and we have reported very smooth surfaces for HfB_2 grown under conditions of extremely low β (10^{-3}−10^{-5}) at 200−300 °C.[33] The lowering of β is also evident from the kinetic data: for the same $Hf(BH_4)_4$ pressure and substrate temperature between 350 and 500 °C, the growth rate of HfN_x-BN film (in the presence of ammonia; Figure 1) is smaller by a factor of 10 than the growth rate of HfB_2 (in the absence of ammonia[13]). As growth temperature increases above 500 °C, the microstructure becomes more columnar and rougher (Figure 7b and c) without a significant change in film composition. This change occurs because of two factors: β for the $Hf(BH_4)_4$ precursor increases with temperature and excess ammonia used should desorb more rapidly from the surface at higher temperatures, thereby reducing its surface coverage and its ability to act as a growth suppressor.[21,22] At all of the growth temperatures reported here, the surface of the HfN_x-BN film is smoother and the microstructure is denser (a larger Hf atomic density as measured by RBS) than for HfB_2 films grown at the same temperature.

(31) Singh, V. K.; Shaqfeh, E. S. G. *J. Vac. Sci. Technol. A-Vac. Surf. Films* **1993**, *11*, 557–568.
(32) Zhao, Y. P.; Drotar, J. T.; Wang, G. C.; Lu, T. M. *Phys. Rev. Lett.* **2001**, *87*, 136102.
(33) Yang, Y.; Jayaraman, S.; Sperling, B.; Kim, D. Y.; Girolami, G. S.; Abelson, J. R. *J. Vac. Sci. Technol. A* **2007**, *25*, 200–206.

All the films grown at 350−800 °C are amorphous as judged from XRD and transmission electron microscopy (TEM) diffraction patterns. A film grown at 450 °C remained amorphous even after being annealed in vacuum at 800 °C for 1 h. We previously reported that amorphous HfB_xN_y films deposited from $Hf(BH_4)_4$ and atomic N showed broad diffraction peaks at positions corresponding to the HfB_2 phase after a 700 °C anneal.[12] Given the relatively low flux of atomic N generated by the remote plasma source, it is possible that those films were deficient in N and contained HfB_2 inclusions. Further experiments would be necessary to determine whether the film growth with atomic N affords a fundamentally different product than with NH_3 due to the surface reaction chemistry or whether the difference reflects the difference in nitrogen flux at the growth surface and is largely independent of the species.

Conclusions

The present results show that ammonia can suppress the deposition of HfB_2 from the single-source molecular precursor $Hf(BH_4)_4$ at temperatures below 350 °C. At higher temperatures, the nanocomposite material HfN_x-BN is formed instead. These effects most likely result from a kinetic competition between different surface reaction channels. Ammonia molecules adsorbed on the growth surface may either (i) reside for a characteristic time, during which they block the adsorption of the precursor and thus reduce the film growth rate, then desorb without decomposition, or (ii) dissociate on the growth surface, which may also change the adsorption rate of the precursor, followed by N incorporation into the film. The suppression effect leads to the growth of highly smooth films, both below and above 350 °C. The resulting nanocomposite HfN_x-BN films are amorphous, resist crystallization up to the maximum temperature tested (800 °C), and are poor electrical conductors.

The results demonstrate that surface chemistry during CVD is a powerful means to control the reactive sticking coefficient and resulting microstructure and complements the usual control parameters of substrate temperature and precursor flux.

Acknowledgment. The authors are grateful to the National Science Foundation for support of this research under grant NSF DMR 04-20768. The authors would like to thank Dr. Yu Yang (a recent Ph.D. graduate of our group) for valuable suggestions and discussions. Compositional and structural analyses of the films were carried out at the Center for Microanalysis of Materials, University of Illinois, which is partially supported by the U.S. Department of Energy under grant DEFG02-91-ER45439.